

# Design of hybrid-core PCF with nearly-zero flattened dispersion and high nonlinearity

Xi Liu (刘 习), Lihong Han (韩利红)\*, Xiaoyu Jia (贾晓宇), Jinlong Wang (王金龙), Fangyong Yu (于方永), and Zhongyuan Yu (俞重远)

State Key Laboratory of Information Photonics and Optical Communications, Beijing University of Posts and Telecommunications, Beijing 100876, China

\*Corresponding author: hanlh.star@gmail.com

Received May 26, 2014; accepted October 24, 2014; posted online December 30, 2014

We present a new structure of nearly-zero flattened dispersion and highly nonlinear photonic crystal fiber (PCF) in the telecommunication window. This fiber design is comprised of a hybrid-core region with bismuth-doped region in the center and three lower bismuth-doped regions in the first ring that enables dispersion control while maintaining a high nonlinear coefficient. Numerical analysis results show that the proposed PCF is achieved with a nonlinear coefficient of about  $3301 \text{ W}^{-1} \text{ km}^{-1}$ , a dispersion value of about  $0.5537 \text{ ps}/(\text{nm}\cdot\text{km})$  at  $1550 \text{ nm}$ , and nearly-zero flattened dispersion fluctuating within  $2.5 \text{ ps}/(\text{nm}\cdot\text{km})$  ranging from  $1.496$  to  $1.596 \mu\text{m}$ .

OCIS codes: 060.5295, 060.4370, 060.2400.

doi: 10.3788/COL201513.010602.

Photonic crystal fiber (PCF), whose cladding contains an array of airholes running along the fiber length, has been widely studied over the past years<sup>[1]</sup>. PCFs are more flexible in structure design than in conventional fibers because of their special structures, so one can choose modest structure parameters of the PCFs to obtain unique optical properties<sup>[2,3]</sup>, such as endlessly single-mode transmission, novel dispersion property<sup>[4]</sup>, high nonlinearity, and high birefringence. Among the properties of PCFs, group-velocity dispersion and nonlinearity are widely studied in PCFs. In particular, highly nonlinear PCFs are suitable candidates for many practical applications in optical communication systems and nonlinear optics. And PCFs with flattened dispersion and high nonlinearity may have a variety of potential applications, such as supercontinuum generation<sup>[5]</sup> and all-optical signal processing<sup>[6]</sup>. Zheng *et al.*<sup>[7]</sup> reported a fiber with a very high nonlinear coefficient and zero dispersion at  $1550 \text{ nm}$  by using the high-index contrast and flexibility of the PCF structure.

PCF based on silica has been investigated extensively to obtain high nonlinearity<sup>[8]</sup>. The enhancement of the effective nonlinear coefficient in PCF is achieved by high confinement of light field in the small core area. Generally, we have two approaches to enhance the fiber nonlinearity: one is to reduce the effective core area and the other is to use a core doped with a glass material of high refractive index. However, the reduction in fiber core diameter may easily cause damage to the fiber end face because of high-power density concentrating in the core area. And the significantly high nonlinearity can be expected in structured fiber with high refractive index glasses. As a result, we can make use of the advantage of high refractive index glass to

obtain high nonlinearity in a simple fiber structure<sup>[9]</sup>. Recently, several kinds of multi-component glass materials have been employed to obtain high nonlinearity, such as lead-silicate<sup>[10]</sup>, chalcogenide<sup>[11]</sup>, tellurite<sup>[12]</sup>, and bismuth-silicate<sup>[13]</sup> glass systems. Among these glasses, the bismuth-oxide glasses show unique properties. The bismuth-oxide glass has not only good transmission capability in a very wide wavelength range, high refractive index ( $n = 1.87\text{--}2.6$ ), and higher nonlinear refractive index ( $n_2 = 3.2 \times 10^{-19}\text{--}1.81 \times 10^{-17} \text{ m}^2/\text{W}$ ) but also has no toxic elements<sup>[14]</sup>. Due to the extremely high refractive index of  $\text{Bi}_2\text{O}_3$ -based glass in optical telecommunication wavelength, one can utilize bismuth-based glass as a fiber core to achieve high optical nonlinearity.

Generally, high refractive index material has a large material dispersion that may cause much larger group-velocity dispersion to high nonlinear fibers made of high refractive index material than silica-based fibers<sup>[15]</sup>. The control of chromatic dispersion in the PCF is an important problem for practical applications. As we know, the total dispersion is composed of the material dispersion and the waveguide dispersion. However, the material dispersion cannot be changed a lot, but we can utilize PCF's special structure to change the waveguide dispersion to adjust the total dispersion. Effect of the waveguide dispersion on the total dispersion depends on the structure parameters of the PCF. Hence, the flexible waveguide structure of PCF offers the possibility to balance the large material dispersion of high refractive index material.

In this letter, we demonstrate a novel PCF structure with a hybrid core<sup>[16]</sup> using the finite element method (FEM) with scattering boundary condition. The hybrid-core region of this fiber design is comprised of two

bismuth-doped materials. The bismuth-doped core region can make high nonlinearity in the PCF. And another three bismuth-doped regions around the core in the first ring and the rest airholes in the cladding can adjust the dispersion property of the PCF. We numerically investigate the influence of the structure parameters of PCF on chromatic dispersion and nonlinear coefficients. Through optimizing the structure parameters of the PCF, we obtain a modest design of PCF with nearly-zero flattened dispersion and high nonlinearity. The nonlinear coefficient is up to  $3301 \text{ W}^{-1} \text{ km}^{-1}$  at  $1550 \text{ nm}$ . Compared with the published results about nonlinear PCFs with flattened dispersion property, such as PCF with the nonlinear coefficient about  $11 \text{ W}^{-1} \text{ km}^{-1}$  at  $1550 \text{ nm}$ <sup>[17]</sup>, PCF with the nonlinear coefficients of about  $29.65 \text{ W}^{-1} \text{ km}^{-1}$  at  $1550 \text{ nm}$ <sup>[18]</sup> and  $226 \text{ W}^{-1} \text{ km}^{-1}$  at  $1550 \text{ nm}$ <sup>[19]</sup>, the nonlinear coefficient in our proposed structure is largely improved.

There are quite many literature studies having calculated the nonlinearity of PCFs. The nonlinear coefficient  $\gamma$ <sup>[20]</sup> of the PCFs can be described by the nonlinear refractive index  $n_2$  as

$$\gamma = \frac{2\pi}{\lambda} \frac{n_2}{A_{\text{eff}}}, \quad (1)$$

where  $\lambda$  denotes the wavelength and the nonlinear refractive index  $n_2$  of the bismuth-doped glass<sup>[21]</sup> is calculated by

$$n_2 = \frac{12\pi^2}{n_1^2 c} \left( \frac{n_1^2 - 1}{4\pi} \right)^2 \times 10^{-10}, \quad (2)$$

where  $n_1$  is the linear refractive index. The effective area  $A_{\text{eff}}$ <sup>[20]</sup> based on the solution of  $E(x, y, z)$  is described as

$$A_{\text{eff}} = \frac{\left( \int_{-\infty}^{\infty} \int_{-\infty}^{\infty} |E|^2 dx dy \right)^2}{\int_{-\infty}^{\infty} \int_{-\infty}^{\infty} |E|^4 dx dy}. \quad (3)$$

Generally, the total dispersion coefficient  $D_T$  can be expressed as the sum of the waveguide dispersion  $D_W$  and the material dispersion  $D_M$ <sup>[22]</sup> as

$$D_T \approx D_W + D_M. \quad (4)$$

The dispersion coefficient is proportional to the second derivatives of mode effective index  $n_{\text{eff}}$  with respect to the wavelength. The definition of dispersion coefficient  $D(\lambda)$  is expressed as

$$D(\lambda) = -\frac{\lambda}{c} \frac{d^2 \text{Re}(n_{\text{eff}})}{d\lambda^2}, \quad (5)$$

where  $c$  is the velocity of light in vacuum,  $\text{Re}(\dots)$  stands for the real part of a physical quantity,  $n_{\text{eff}}$  is the effective mode index,  $D(\lambda)$  is the total dispersion as mentioned above. The material dispersion given by Sellmeier's formula is directly included in the calculation. It is possible to alter the balance between the two dispersion mechanisms and one can achieve a desired dispersion profile.

We know that it is difficult to achieve a highly nonlinear PCF at  $1550 \text{ nm}$  and keep the dispersion flattened

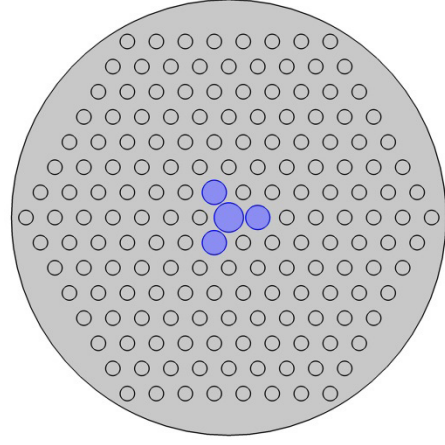


Fig. 1. Cross-section view of the PCF structure. The blue regions are doped materials.

over a broad wavelength range when using a conventional PCF with all the same airhole diameters in the cladding region. Here, we propose a novel PCF structure with a three-fold symmetric hybrid-core region and the same airhole diameters.

The cross-section view of the PCF structure is shown in Fig. 1. The hybrid-core region is composed of a bismuth-doped center region surrounded by another three bismuth-doped regions embedded in a standard triangular air/pure silica cladding structure. The refractive index of the air is 1 and the refractive index of the silica is given by Sellmeier's formula considering the material dispersion. We have chosen a high  $\text{Bi}_2\text{O}_3$ -content glass (ABH160) which contains 65.5 mol% of  $\text{Bi}_2\text{O}_3$  used as the fiber-core medium and another a lower  $\text{Bi}_2\text{O}_3$ -content glass (B037) which contains 55.0 mol% used as three doped regions around the fiber core<sup>[21]</sup>. The refractive indices of ABH160 and B037 are 2.219 and 2.215 at  $1550 \text{ nm}$ , respectively. The material dispersion of the bismuth-doped glasses can be calculated by

$$D_M = -\frac{\lambda}{c} \frac{d^2 n(\lambda)}{d\lambda^2}, \quad (6)$$

where  $n(\lambda)$  is fitted by a polynomial as<sup>[21]</sup>

$$n^2(\lambda) = 1 + \frac{A_1}{1/a_1^2 - 1/\lambda^2} - A_2 \lambda^2. \quad (7)$$

The fitting parameters are listed in Table 1.

As shown in Fig. 1, we can see the PCF is designed with 7-layer rings of airholes, because the ring number is important for confinement loss during the design procedure. The diameter of the circular doped region

**Table 1.** Fitting Parameters of ABH160 and B027

Doped Glass	$a_1$ (nm)	$A_1$	$A_2$
ABH160	210.1	$8.746 \times 10^{-5}$	$5.20 \times 10^{-9}$
B027	200.2	$8.609 \times 10^{-5}$	$2.10 \times 10^{-9}$

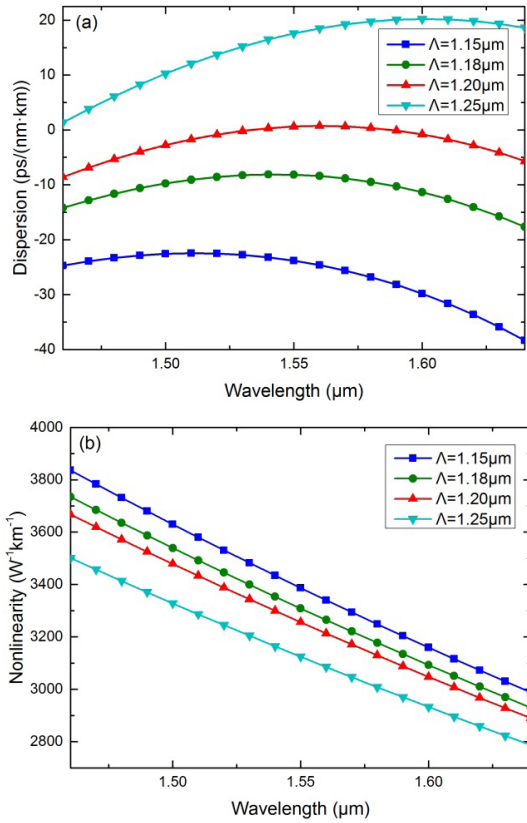


Fig. 2. (a) Dispersion and (b) nonlinear coefficients of the PCF with  $d_0/\Lambda = 1$ ,  $d_1/\Lambda = 0.835$ , and  $d/\Lambda = 0.5$  by varying  $\Lambda$ .

in the fiber core is  $d_0$  and  $\Lambda$  denotes lattice constant. The first ring surrounding the doped fiber core has three small airholes and three big doped regions with diameters  $d$  and  $d_1$ , respectively. All of the airholes in the structure are provided with the same diameters  $d$ . The validation of the design is achieved by using an efficient full-vector FEM with boundary scattering condition for accurate modeling of PCF. So we can obtain the complex eigenvalues as well as the mode profiles. The proposed structure can maintain single-mode transmission. The fundamental mode has three-fold symmetry due to the symmetric property of the core. The three bismuth-doped regions in the first ring reduce the relative refractive index difference between the core and cladding can make the mode extended into the cladding region and the surrounding airholes around the fiber core can make the mode bounded in the core region. So the diameters of the first ring become the key design parameters in numerical simulation, affecting the optical properties remarkably. In the following, some optimized structure parameters are searched out in PCF design process and are shown in detail.

We use a full-vector FEM in simulation of the fiber structure to calculate the field distribution and its fundamental mode effective refractive index. And then we obtain the nonlinear coefficient and dispersion curves versus wavelength calculated by Eqs. (1) and (5). The wavelength range in the simulation is between 1.46 and 1.64  $\mu\text{m}$ . We mainly focus on the effects of the doped

core diameter  $d_0$ , the doped region diameters  $d_1$  in the first ring, the airhole diameter  $d$ , and the pitch  $\Lambda$  on the dispersion properties and nonlinear coefficient. Firstly, we fix the structure parameters  $d_0/\Lambda = 1$ ,  $d_1/\Lambda = 0.835$ , and  $d/\Lambda = 0.5$  in PCF, and then vary the value of  $\Lambda$  to discuss the changes in dispersion and nonlinear coefficients versus wavelength  $\lambda$  (Figs. 2(a) and (b)). From the dispersion curves in Fig. 2(a), we can observe that the dispersion value of each curve increases in the short-wavelength range and decreases in the long-wavelength range as the wavelength  $\lambda$  increases. It means that the dispersion slope changes from positive value to zero and then from zero the negative value, so we can get a zero-dispersion slope wavelength point. We can also conclude that the dispersion curves increase with the value of  $\Lambda$  increasing in the current wavelength range and the zero-dispersion slope wavelength of the curves shift to long-wavelength side with the  $\Lambda$  increasing. Therefore, a suitable  $\Lambda$  is very important in adjusting the dispersion curve. It is obvious that the dispersion profile of the PCF with  $\Lambda = 1.2 \mu\text{m}$  is very close to the zero flattened dispersion around 1550 nm as expected. So we can keep this preliminary design about nearly-zero flattened dispersion as a reference point in the following discussion. As shown in Fig. 2(b), the nonlinear coefficient values are very high and decrease gradually with  $\Lambda$  increasing. The bismuth-doped fiber core makes the PCF obtain high nonlinearity because of the high nonlinear refractive index of the doped material.

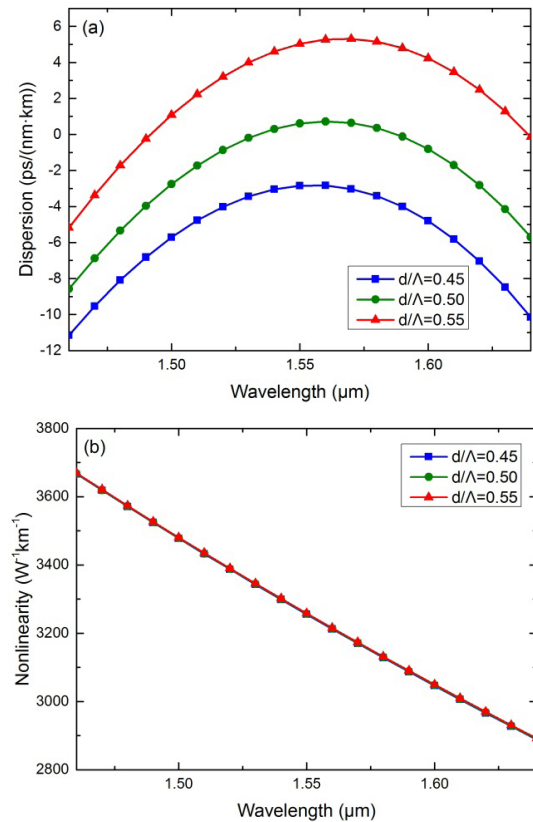


Fig. 3. (a) Dispersion and (b) nonlinear coefficients of the PCF with  $\Lambda = 1.2 \mu\text{m}$ ,  $d_0/\Lambda = 1$ , and  $d_1/\Lambda = 0.835$  by varying  $d/\Lambda$ .

When  $\Lambda = 1.2 \mu\text{m}$  in this case, the nonlinear coefficient is up to  $3256 \text{ W}^{-1} \text{ km}^{-1}$  at  $1550 \text{ nm}$ .

Next, we keep the structure parameters  $\Lambda = 1.2 \mu\text{m}$ ,  $d_0/\Lambda = 1$ , and  $d_1/\Lambda = 0.835$  in PCF and change airhole diameter  $d$  to investigate the influence of this parameter on dispersion and nonlinear coefficients for PCF. The numerical results are illustrated in Figs. 3(a) and (b). We can find that the dispersion curves increase with the diameter  $d$  increasing for the whole wavelength range because the refractive index difference between the core and the cladding increases when the  $d$  increases. Besides, we can observe that the zero-dispersion slope wavelength of the curves shift slightly to the long-wavelength side with the  $d$  increasing. We can see from Fig. 3(b), all of the nonlinear coefficient curves nearly coincide with each other. For  $1550 \text{ nm}$ , the  $d/\Lambda$  changes from  $0.45$  to  $0.55$  and the nonlinear coefficients are  $3255$ ,  $3256$ , and  $3258 \text{ W}^{-1} \text{ km}^{-1}$ , respectively. That is because the highly doped core makes the mode tightly bounded in the core region and the influence of airholes on the nonlinear coefficient is very less.

The three doped regions around the fiber core can largely change the refractive index difference between the core and the cladding. Here we fix  $\Lambda = 1.2 \mu\text{m}$ ,  $d_0/\Lambda = 1$ , and  $d/\Lambda = 0.5$  and study the influence of  $d_1$  on dispersion and nonlinear coefficients. As shown in Fig. 4(a), we can observe that  $d_1$  has a large influence on the dispersion values. The dispersion curves decrease with the

diameter  $d_1$  increasing for the whole wavelength range. The reason is that the light confinement ability within the core region is weakened when  $d_1$  increases, affecting the dispersion value severely. Besides, the zero-dispersion slope wavelength of the curves shift slightly to the short-wavelength side with the  $d_1$  increasing, indicating that  $d_1$  has a very less influence on the shift of the zero-dispersion slope wavelength. According to Fig. 4(b), we can observe that the nonlinear coefficient decreases with the  $d_1$  increasing. The mode in the fiber core extends to the cladding with  $d_1$  increasing and the effective mode area increases. From Eq. (1), we find that the nonlinear coefficient decreases as the effective mode increases. For  $1550 \text{ nm}$ , the  $d_1/\Lambda$  changes from  $0.825$  to  $0.845$  and the nonlinear coefficients are  $3273$ ,  $3256$ , and  $3238 \text{ W}^{-1} \text{ km}^{-1}$ , respectively.

The diameter  $d_0$  of the doped core region in PCF is very important in PCF design process. Here we fix structure parameters  $\Lambda = 1.2 \mu\text{m}$ ,  $d/\Lambda = 0.5$ , and  $d_1/\Lambda = 0.835$  and the calculated dispersion and nonlinear coefficient curves are illustrated in Figs. 5(a) and (b). From Fig. 5(a), we can observe that the dispersion curves decrease in the short-wavelength side and increases in the long-wavelength side with the  $d_0$  increasing. Moreover, as the  $d_0$  increases, the dispersion value in the zero-dispersion slope wavelength increases slightly and the zero-dispersion slope wavelength of the curves shift to long-wavelength side. From Fig. 5(b), we can observe that the nonlinear

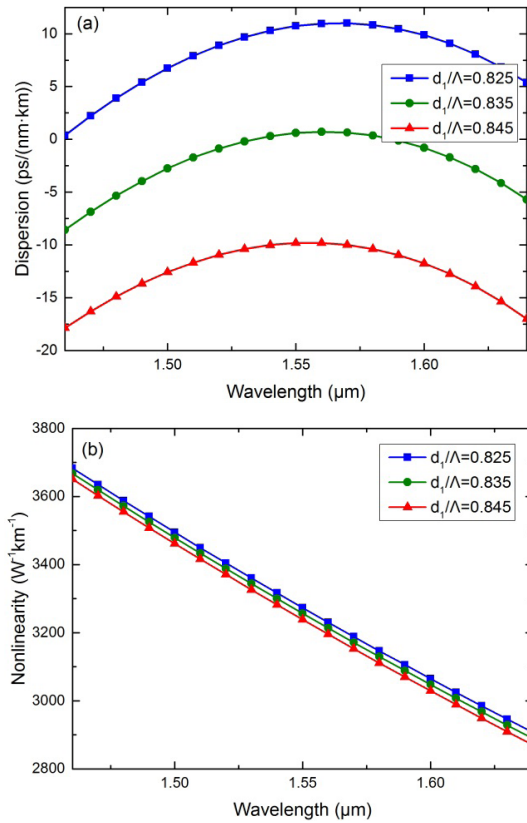


Fig. 4. (a) Dispersion and (b) nonlinear coefficients of the PCF with  $\Lambda = 1.2 \mu\text{m}$ ,  $d_0/\Lambda = 1$ , and  $d/\Lambda = 0.5$  by varying  $d_1/\Lambda$ .

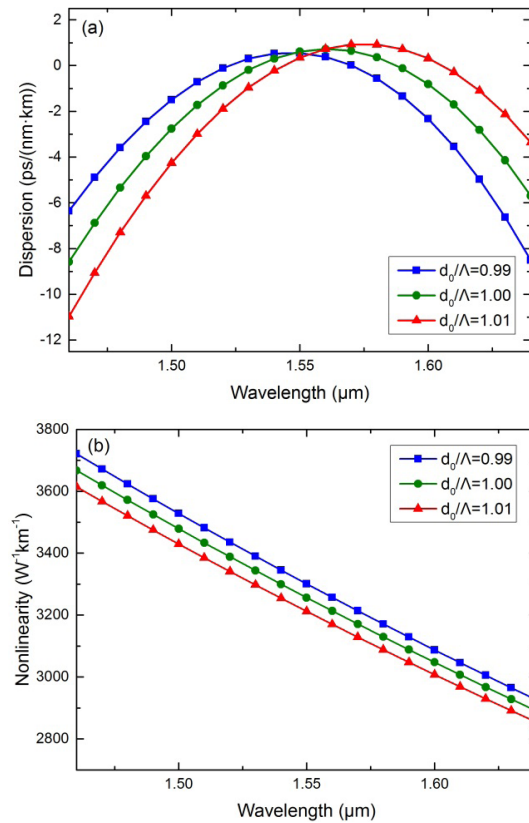


Fig. 5. (a) Dispersion and (b) nonlinear coefficients of the PCF with  $\Lambda = 1.2 \mu\text{m}$ ,  $d/\Lambda = 0.5$ , and  $d_1/\Lambda = 0.835$  by varying  $d_0$ .

coefficient values decrease gradually with the  $d_0$  increasing. That's because the increase of  $d$  leads to a larger effective mode area and the nonlinear coefficient is inversely proportional to the effective mode area. For 1550 nm, the  $d_0/\Lambda$  changes from 0.99 to 1.01 and the nonlinear coefficients are 3301, 3256, and 3212  $\text{W}^{-1} \text{km}^{-1}$ , respectively.

Based on the numerical analysis above, we can obtain an optimized PCF structure with nearly-zero flattened dispersion and high nonlinearity by selecting the parameters  $\Lambda = 1.2 \mu\text{m}$ ,  $d/\Lambda = 0.5$ ,  $d_1/\Lambda = 0.835$ , and  $d_0/\Lambda = 0.99$ . In this design, the dispersion value is about 0.5537 ps/(nm·km) and the nonlinear coefficient is up to 3301  $\text{W}^{-1} \text{km}^{-1}$  at 1550 nm. The dispersion fluctuation is between 0.57 and  $-1.93$  ps/(nm·km) in the wavelength range from 1.495 to 1.595  $\mu\text{m}$ . We find that the 1% fluctuation in diameter of doped core has less influence on dispersion and not much influence on nonlinearity at 1550 nm. The 1% fluctuation in diameter of doped region in the first ring has an influence of about 8 ps/(nm·km) variation on dispersion and less influence on nonlinearity at 1550 nm. The 5% fluctuation in diameter of airhole has less influence on both dispersion and nonlinearity at 1550 nm. And the 1% fluctuation in value of pitch  $\Lambda$  has an influence of about 5 ps/(nm·km) variation on dispersion and not much influence on nonlinearity at 1550 nm. We can take these information into account during fabrication.

In conclusion, we propose a hybrid-core PCF with nearly-zero flattened dispersion and high nonlinearity in the 1550 nm telecommunication window. We present the influence of the structure parameters of the designed PCF on dispersion and nonlinear coefficients. By selecting proper structure parameters, we can obtain a PCF with desired dispersion flatten profile and high nonlinearity. The numerical simulations demonstrate that the dispersion value of the designed PCF is about 0.5537 ps/(nm·km) and the nonlinear coefficient is up to 3301  $\text{W}^{-1} \text{km}^{-1}$  at 1550 nm. And we achieve a flattened dispersion profile fluctuating between 0.57 and  $-1.93$  ps/(nm·km) over a wavelength range between 1.496 and 1.596  $\mu\text{m}$ . This PCF with nearly-zero flattened dispersion and high nonlinearity can be properly used in various potential applications, such as supercontinuum generation, all-optical signal processing, and other research and application fields.

This work was supported by the National "863" Program of China under Grant No. 2013AA031501.

## References

1. B. Sévigny, O. Vanvincq, C. Valentin, N. Chen, Y. Quiquempois, and G. Bouwmans, *Opt. Express* **21**, 30859 (2013).
2. J. Zheng, Y. Yu, C. Du, P. Yan, M. Pan, J. Wang, and Z. Liu, *Chin. Opt. Lett.* **10**, S20611 (2012).
3. W. Liang, N. Liu, Z. Li, and P. Lu, *Chin. Opt. Lett.* **11**, S20604 (2013).
4. J. Zhao, J. Hou, C. Yang, Z. Zhong, Y. Gao and S. Chen, *Chin. Opt. Lett.* **12**, S10607 (2014).
5. Z. Holdynski, M. Napierala, M. Szymanski, M. Murawski, P. Mergo, P. Marc, L. R. Jaroszewicz, and T. Nasilowski, *Opt. Express* **21**, 7107 (2013).
6. J. Hou, J. J. Zhao, C. Y. Yang, Z. Y. Zhong, Y. H. Gao, and S. P. Chen, *Photon. Res.* **2**, 59 (2014).
7. L. Zheng, X. Zhang, X. Ren, H. Ma, L. Shi, Y. Wang, and Y. Huang, *Chin. Opt. Lett.* **9**, 040601 (2011).
8. K. Saitoh and M. Koshiba, *Opt. Express* **12**, 2027 (2004).
9. T. Sun, G. Kai, Z. Wang, S. Yuan, and X. Dong, *Chin. Opt. Lett.* **6**, 93 (2008).
10. M. A. Ettabib, L. Jones, J. Kakande, R. Slavik, F. Parmigiani, X. Feng, F. Poletti, G. M. Ponzio, J. D. Shi, M. N. Petrovich, W. H. Loh, P. Petropoulos, and D. J. Richardson, *Opt. Express* **20**, 1629 (2012).
11. W. Q. Gao, M. E. Amraoui, M. S. Liao, H. Kawashima, Z. C. Duan, D. H. Deng, T. L. Cheng, T. Suzuki, Y. Messaddeq, and Y. Ohishi, *Opt. Express* **21**, 9573 (2013).
12. H. H. Cheng, Z. Q. Luo, C. C. Ye, Y. Z. Huang, C. Liu, and Z. P. Cai, *Appl. Opt.* **52**, 525 (2013).
13. T. Hasegawa, *Opt. Commun.* **285**, 3939 (2012).
14. C. Jin, L. Rao, J. H. Yuan, X. W. Shen, and C. X. Yu, *Optoelectron. Lett.* **7**, 194 (2011).
15. T. Hasegawa and S. Ohara, in *Proceedings of Optical Fiber Communication Conference and National Fiber Optic Engineers Conference OThK2* (2009).
16. M. Chen and S. Xie, *Opt. Commun.* **281**, 2073 (2008).
17. K. P. Hansen, *Opt. Express* **11**, 1503 (2003).
18. J. F. Liao, J. Q. Sun, Y. Qin, and M. D. Du, *Opt. Fiber Technol.* **19**, 468 (2013).
19. J. F. Liao, J. Q. Sun, M. D. Du, and Y. Qin, *IEEE Photon. Technol. Lett.* **26**, 1041 (2014).
20. G. Agrawal, *Nonlinear Fiber Optics* (Academic Press, 1995).
21. T. Hasegawa, T. Nagashima, and N. Sugimoto, *Opt. Commun.* **281**, 782 (2008).
22. D. Gloge, *Appl. Opt.* **10**, 2442 (1971).